Antitumor Activity of Ethyl Acetate Extraction of *Wikstroemia chamaedaphne*: Cell Cycle Arrest and Apoptosis-Inducing Activity in Melanoma Cells

Yuan Li [1,3], Chunyan Zhang [3], Yiwen Nie [1,3], Ruifeng Zhang [2,3,4], Xiaoxiang Zhai [4], Yanjuan Duan [4], Wei Fan [1], Weiying Gu [1], Kourong Shi [1], Lan Luo [1*] and Jianyong Zhu [2,3*]

[1] *Department of Pharmacy, Seventh People's Hospital of Shanghai University of Traditional Chinese Medicine, Shanghai 200137, P. R. China*

[2] *Clinical Laboratory Medicine Center, Yueyang Hospital of Integrated Traditional Chinese and Western Medicine, Shanghai University of Traditional Chinese Medicine, Shanghai 200437, P. R. China*

[3] *Central Laboratory, Seventh People's Hospital of Shanghai University of Traditional Chinese Medicine, Shanghai200137, P. R. China*

[4] *Department of Dermatology, Seventh People's Hospital of Shanghai University of Traditional Chinese Medicine, Shanghai 200137, P. R. China*

Abstract: The ethyl acetate extraction (WCE) of *Wikstroemia chamaedaphne* Meisn on the viability of melanoma cell lines B16 and A375 were evaluated. The WCE exhibited a potent cytotoxic against B16 and A375 with IC_{50} values of 156.2 and 192.8 μg/mL, respectively. Cell migration was assessed using a wound healing assay. The WCE caused cell cycle arrest in the G_0/G_1 phase in B16 cells and the S phase in A375 cells, according to cell cycle analysis. Flow cytometric analysis revealed that WCE promoted apoptosis in B16 and A375 cells in a dose-dependent manner. Chemical analysis of WCE resulted in the isolation of a new diterpenoid, wikstchalin A (**6**) with five known flavonoids (**1–5**) and two known diterpenoids (**7** and **8**). Spectroscopic analysis revealed their structures, and CD analysis revealed the absolute configurations of **6**. The absolute structure of pimelotide A (**7**) was firstly confirmed by single-crystal X-ray diffraction. The cytotoxicities of all the compounds (**1−8**) were evaluated against B16 cell lines. Compound **8** was more active than the positive control, dacarbazine (IC_{50} 300 μM), in terms of cytotoxicity against B16, with an IC_{50} value of 7.9 μM.

Keywords: *Wikstroemia chamaedaphne*; flavonoid; diterpenoid; antitumor activity © 2022 ACG Publications. All rights reserved.

1. Introduction

Malignant melanoma is one of the most common malignancies. Around 232100 cases of all newly diagnosed primary malignant cancers are cases of cutaneous melanoma, and there are 55500 newly

---

* Corresponding author: E-Mail: ll4820703@163.com, jyzhu@foxmail.com ;Phone:086-021-58670561

deaths worldwide every year [1]. Malignant melanoma is frequently resistant to chemotherapy and radiotherapy, and advanced melanoma patients have a dismal prognosis, with a median overall survival of 8-10 months and a 5-year survival rate of 6% [2]. Metastatic melanoma is one of the most difficult tumors to treat, imposing a financial burden on both individual patients and society. Despite major breakthroughs in chemotherapy regimens, there has been little change in malignant melanoma mortality during the last several decades. The finding of exact molecular targets for malignant melanoma chemoprevention is believed to be an accessible option for the development of new preventive medicines.

Wikstroemia chamaedaphne Meisn., a toxic shrub native to China, has been used in traditional Chinese medicine to treat edema, cough, hepatitis, schizophrenia, and infertility [3]. Previous chemical investigations on the *W. chamaedaphne* have resulted the isolation of daphnane diterpenoids [4-6], flavonoids [5], and phenolic constituents [7]. As part of our screening program to investigate antineoplastic compounds from this genus [8], ethyl acetate extraction (WCE) of *W. chamaedaphne* demonstrated cytotoxic activity. The WCE was tested for cytotoxicity against two melanoma cell lines, B16 and A375, respectively. The WCE was found to be moderate activity to the melanoma cell lines B16 and A375, with IC_{50} values of 156.2 and 192.8 μg/mL, respectively. Chemical investigation of WCE has led to the isolation of a new wikstchalin A (**6**) with the five known flavonoids (**1–5**) and two known diterpenoids (**7 and 8**). Spectroscopic analysis revealed their structures, and CD analysis revealed the absolute configurations of **6**. The absolute structures of pimelotide A (**7**) were firstly confirmed by single-crystal X-ray diffraction. Herein, details of cytotoxic activities of WCE, the isolation, and structural elucidation are described.

2. Materials and Methods

2.1. General Methods

At 25°C, NMR spectra were collected using a Bruker AM-600 spectrometer. A semi-preparative HPLC Eclipse XDB-C_{18} column was used in conjunction with an Agilent 1200 series HPLC system. For column chromatography (CC), we used a silica gel (300-400 mesh, Qingdao Haiyang Chemical Co., Ltd.), a C_{18} reversed-phase silica gel (12 nm, S-50 μm, YMC Co., Ltd.), and a Sephadex LH-20 gel (Amersham Biosciences). All of the solvents were analytical or chromatographic grade (Shanghai J&K Scientific Ltd or Chemical Reagents Company, Ltd.).

2.2. Plant Material

W. chamaedaphne flower buds were purchased from Bozhou Jinwan Pharmaceutical Company (Bozhou, People's Republic of China) and collected in November 2019 from Taiyuan, Shanxi Province, People's Republic of China. One of the authors (L. Luo) identified the specimen. A standard sample (SWCZ-201911) was deposited at the Central Laboratory, Seventh People's Hospital of Shanghai University of TCM.

2.3. Extraction and Isolation

The air-dried powder of *W. chamaedaphne* flower buds (10 kg) were extracted three times with 95% EtOH (60 L, one month each) at room temperature, and yielding a crude extract (1.2 kg) upon removal of the solvent. The extract was suspended in 3 L of water and partitioned three times with petroleum ether (PE, 3 L), ethyl acetate (EtOAc, 3 L), and n-butanol (3 L) to yield three corresponding portions.The ethyl acetate extract (300 g) was separated using an XDA-7 macroporous resin with EtOH−H_2O (30% to 100%) to yield three fractions, *Fr. A−Fr. C*. Then, *Fr. C* (80 g) was passed through a silica gel (PE/EtOAc, 1:0 → 0:1, v/v) to give *Fr. C1–Fr. C4*. *Fr. C1* (6.0 g) was loaded onto Sephadex LH-20 column and eluted with CH_2Cl_2-MeOH (1:1) led to *Fr. C1a−Fr. C1c*. *Fr. C1a* was purified by semi-preparative HPLC Agilent Eclipse XDB-C_{18} column (5 μM, 250 × 9.4 mm, MeOH/H_2O, 9:1, 3 mL/min), to afford **6** (10 mg, t_R 11 min), **7** (15 mg, t_R 13 min), and **8** (7 mg, t_R 15 min). *Fr. C4* was

separated over a Sephadex LH-20 column with EtOH to yield four fractions (*C4a−C4d*). *Fr. C4d* was purified by semi-preparative HPLC (Eclipse XDB-C$_{18}$ column, MeOH/H$_2$O, 7:3, 3 mL/min) to afford **4** (9 mg, t_R 8 min) and **5** (50 mg, t_R 9 min). *Fr. B* was separated over a Sephadex LH-20 column with CH$_2$Cl$_2$/MeOH (1:1) into two fractions (B1 and B2). *Fr. B2* was also purified by a semi-preparative HPLC (Eclipse XDB-C$_{18}$ column, MeOH/H$_2$O, 6:4, 3 mL/min), to afford **1** (7 mg, t_R 10 min), **2** (9 mg, t_R 11 min), and **3** (11.1 mg, t_R 12 min).

Wikstchalin A (**6**): a white powder; $[\alpha]^{25}_D$ −101.1 (*c* 0.1, MeOH); UV (MeOH) λmax (log ε) 195 (3.10) nm, 232 (3.21); ECD (*c* 1.0×10^{-4} M, MeOH) λ_{max} ($\Delta\varepsilon$) 235 (−5.61), 195 (+18.15) nm; IR (KBr) ν_{max} 3364, 2926,1698,1681,1633, 1449, 1014, 734, and 524 cm^{-1}; ^{1}H and ^{13}C NMR data, see Table 1; HRESIMS m/z 331.1926 [M − H]$^-$ (calcd for C$_{20}$H$_{27}$O$_4$, 331.1915).

X-ray crystallographic study of pimelotide A (**7**): C$_{30}$H$_{42}$O$_9$ (M =546.28 g/mol): monoclinic, space group P21 (no. 4), a = 19.2720(8) Å, b = 7.6596(3) Å, c = 20.3311(8) Å, β = 107.728 (2) °, V = 2858.7(2) Å3, Z = 4, T = 192.99 K, μ(GaKα) = 0.508 mm^{-1}, Dcalc = 1.307 g/cm3, 53958 reflections measured (6.592° ≤ 2Θ ≤ 109.9°), 10767 unique (Rint = 0.0558, Rsigma = 0.0445) which were used in all calculations. The final R1 was 0.0543 (I > 2σ(I)) and wR2 was 0.1584. Absolute structure parameter = 0.13(8). Crystallographic data of **7** have been deposited in the Cambridge Crystallographic Data Centre (deposition number: CCDC 2092946).

2.4. Cell Culture

B16 mouse malignant melanoma and A375 human malignant melanoma cells were provided by the cell bank of the Chinese Academy of Sciences (Shanghai, China). B16 cells were thawed and grown in RPMI-1640 and supplemented with 0.5% penicillin/streptomycin and 10% FBS, while A375 cells were thawed and expanded in DMEM. The cells were incubated at 37 °C with 5% CO$_2$. For the following assays, all cells were harvested during the exponential growth phase.

2.5. Cell Viability Assay

The 3-(4,5-dimethylthiazol-2-yl)-2,5-diphenyltetrazolium bromide (MTT) assay was used to determine cell viability. Separately, B16 and A375 cells were seeded into 96-well plates at a density of 5×10^3 cells/well and incubated overnight. Following a 24-hour incubation with WCE extract at various concentrations, B16 and A375 cells were treated with MTT (5 mg/mL dissolved in PBS) for an additional 4-hour incubation at 37 °C. Following the dissolution of the formazan crystals in DMSO, the absorbance at 560 nm was measured with a spectrophotometer and the IC$_{50}$ was calculated using GraphPad 8. All assays were carried out in triplicate.

2.6. Morphological Analysis

The AO/PI staining assay was used to investigate the morphological changes that occurred in the cells after WCE treatment. For 24 hours, cells were treated with 100, 200, 300, and 400 μg/mL of WCE, respectively. 300 μM of dacarbazine (DBZ) were used as positive controls. Acridine orange (AO) and propidium iodide were used to stain B16 and A375 cells (PI). The plate was incubated in the dark for 5 minutes before being washed with PBS to remove the unbound dye. An EVOS FL digital microscope (200 objective) was used to capture the cell morphology. All assays were carried out in triplicate.

2.7. Wound Healing Assay

B16 and A375 cells (1×10^6 cells/well) were seeded and incubated until the plates were full. To assess cell migration, wound lines in the shape of a cross were made in confluent cells by scraping with a plastic 200 μL pipette tip. After wounding, floating cells were washed with PBS and cultured for 48 hours in 2 percent FBS-containing DMEM or RPMI-1640 supplemented with or without WCE. Data

were collected as previously described [9]. Specifically, under a microscope, the width of the wound healing was then observed and photographed. All assays were carried out in triplicate.

2.8. Cell Cycle Analysis

B16 and A375 cells were harvested and washed twice with cold PBS after 24 hours of WCE or DBZ treatment. The cells were fixed overnight in 75% frozen ethanol at 4°C before being resuspended in 1 mL cold PBS. After adding 500 μL of dye solution, the cells were incubated in the dark at room temperature for 30 minutes before being detected by flow cytometry. All assays were carried out in triplicate.

2.9. Cell Apoptosis Analysis

The effect of WCE on cell apoptosis was investigated using Annexin V-FITC apoptosis detection in conjunction with flow cytometry. For 24 hours, B16 and A375 cells were treated with varying doses of WCE or DBZ. After washing with PBS, cells at a concentration of 5×10^4 cells/mL were gently mixed with 5 μL Annexin V-FITC and 5 μL PI. Cells were then left at room temperature in the dark for 15 minutes. The cells were then placed in 400 μL binding buffer before being loaded onto the FACS Calibur. FLOW JO 10 was used for additional analysis. As controls, cells were left untreated or stained with Annexin V-FITC or PI alone. All assays were carried out in triplicate.

3. Results and Discussion

3.1. Cytotoxic Effects of WCE Against Melanoma Cells

An MTT assay was used to assess the WCE's in vitro cytotoxicity against B16 and A375 melanoma cell lines *in vitro*. WCE was found to have significant cytotoxic effects against B16 and A375, with IC$_{50}$ values of 156.2 and 192.8 μg/mL after 24 hours of treatment, respectively (Figure 1).
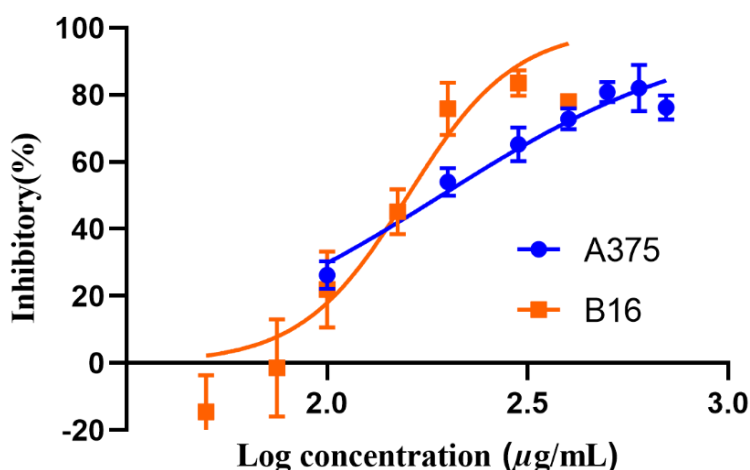

Figure 1. The WCE inhibited the melanoma cells proliferation *in vitro*. The cell viability of A375 and B16 after WCE treated for 24 h in MTT assay

3.2. Morphological Changes in Melanoma Cells Treated with WCE

To confirm the apoptosis-inducing effects of WCE, melanoma cells were examined in fluorescence photomicrographs of B16 and A375 cells stained with acridine orange (AO) after treatment with various concentrations of WCE for 24 hours. After that, the inverted light or fluorescence microscope was used to examine the morphological features of apoptosis. The cells in the control group had normal morphology and were stained green in the nuclei. When the WCE concentration was

between 100 and 200 μg/mL, the cell membrane shrank and the nuclear chromatin started to pyknosis, indicating the early manifestation of apoptosis. Most of the nuclei were yellow green and bead-like when the WCE concentration was 300 μg/mL, and the nuclear chromatin was orange red and pyknosis, indicating that many of the cells had entered the late stage of apoptosis. When the WCE concentration was raised to 400 μg/mL, the cell membrane ruptured and the nucleus turned red (Figure 2). Thus, WCE could cause apoptosis in B16 and A375 cells in a dose-dependent manner.
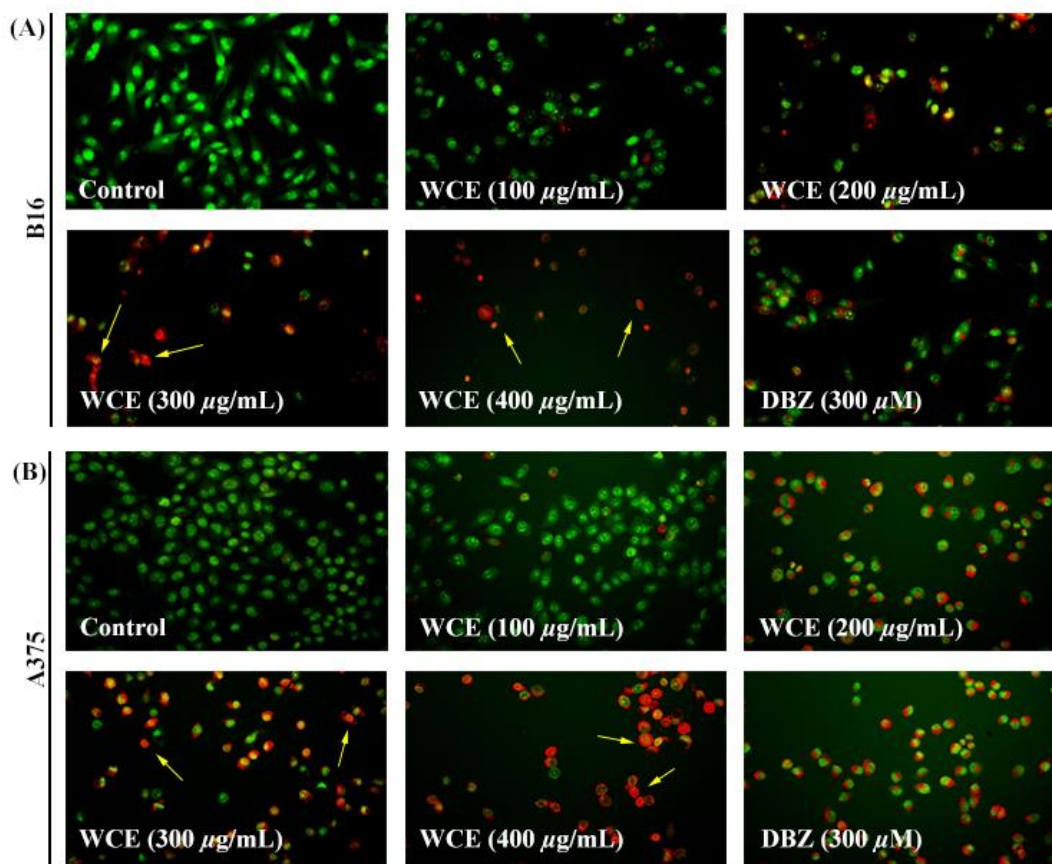

Figure 2. Evaluation of the effects of WCE on apoptosis. (A) A375 cells treated with the different concentrations of WCE and DBZ for 24 h. (B) B16 cells were treated for 24 hours with various concentrations of WCE and DBZ. AO/ PI was used to stain the cells. Representative images of the compound's apoptosis effects (200 $\times$ magnification), with yellow arrows highlighting apoptotic cells.

3.3. Antimigratory Activity of the WCE in Melanoma Cells

Wound-healing assays were used to investigate the effects of WCE on melanoma cell migration. B16 and A375 cells were treated with different concentrations of WCE for a total of 48 hours to see how it affected migration. The wound was measured in width after incubation and compared to the original ones. WCE's anti-migration activity was assessed using this method of analysis. In B16 and A375 cells, the WCE has equivalent activity to the positive control DBZ (Figure 3).
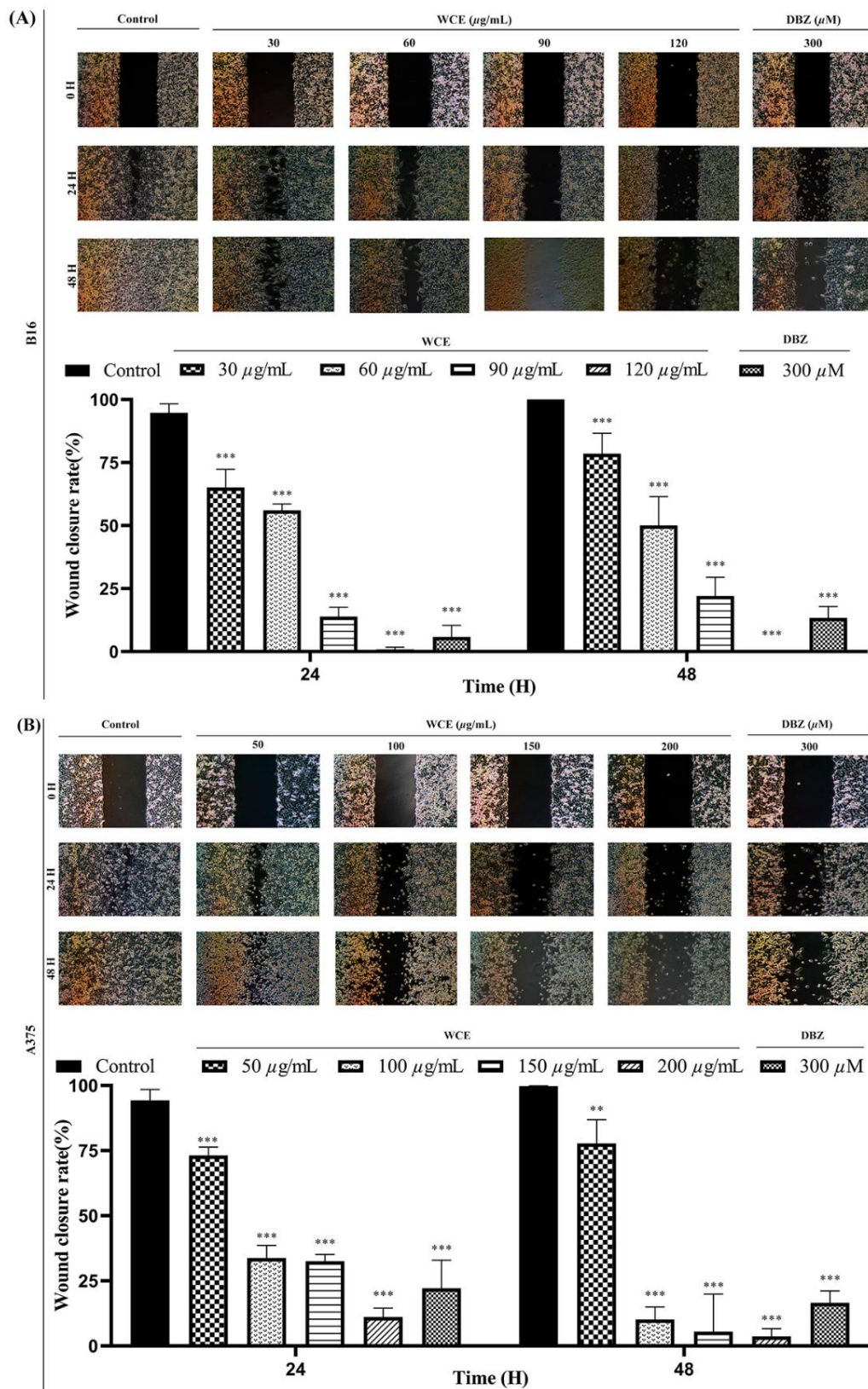
Figure 3. Wound-healing assays by different concentrations of WCE and DBZ with B16 cells and A375 cells. (A) Wound-healing assay in B16 cells. (B) Wound-healing assay in A375 cells. ∗∗p < 0.01 and ∗∗∗p < 0.001 vs control group

3.4. The WCE Induce Cell Cycle Arrest in B16 and A375 Melanoma Cells

The cell cycle profiles of B16 and A375 cells were analyzed using flow cytometry to further investigate the effects of WCE on the cell cycle. The cells were stained with PI after being treated with WCE at concentrations of 100, 200, 300, and 400 μg/mL for 48 hours. The cells were then flow cytometrically examined to determine their DNA content. When the concentration of WCE was increased, the percentage of cells in G_0/G_1 phase increased from 58.94% to 59.45%, 62.37%, 69.41 %, and 80.41 %, respectively, while the number of cells in S and G_2/M phase decreased gradually (Figure 4A), indicating that WCE could block the cell cycle in G_0/G_1 phase to inhibit B16 cell proliferation. The percentage of cells in the S phase increased significantly after WCE treatment, while the percentage of cells in the G_0/G_1 and G_2/M phases decreased significantly (Figure 4B). S phase values increased from 23.14% to 31.17%, 43.05%, 45.17%, and 45.63%, respectively, when compared to the control group, indicating that WCE could block the cell cycle in S phase to inhibit the proliferation of A375 cells.
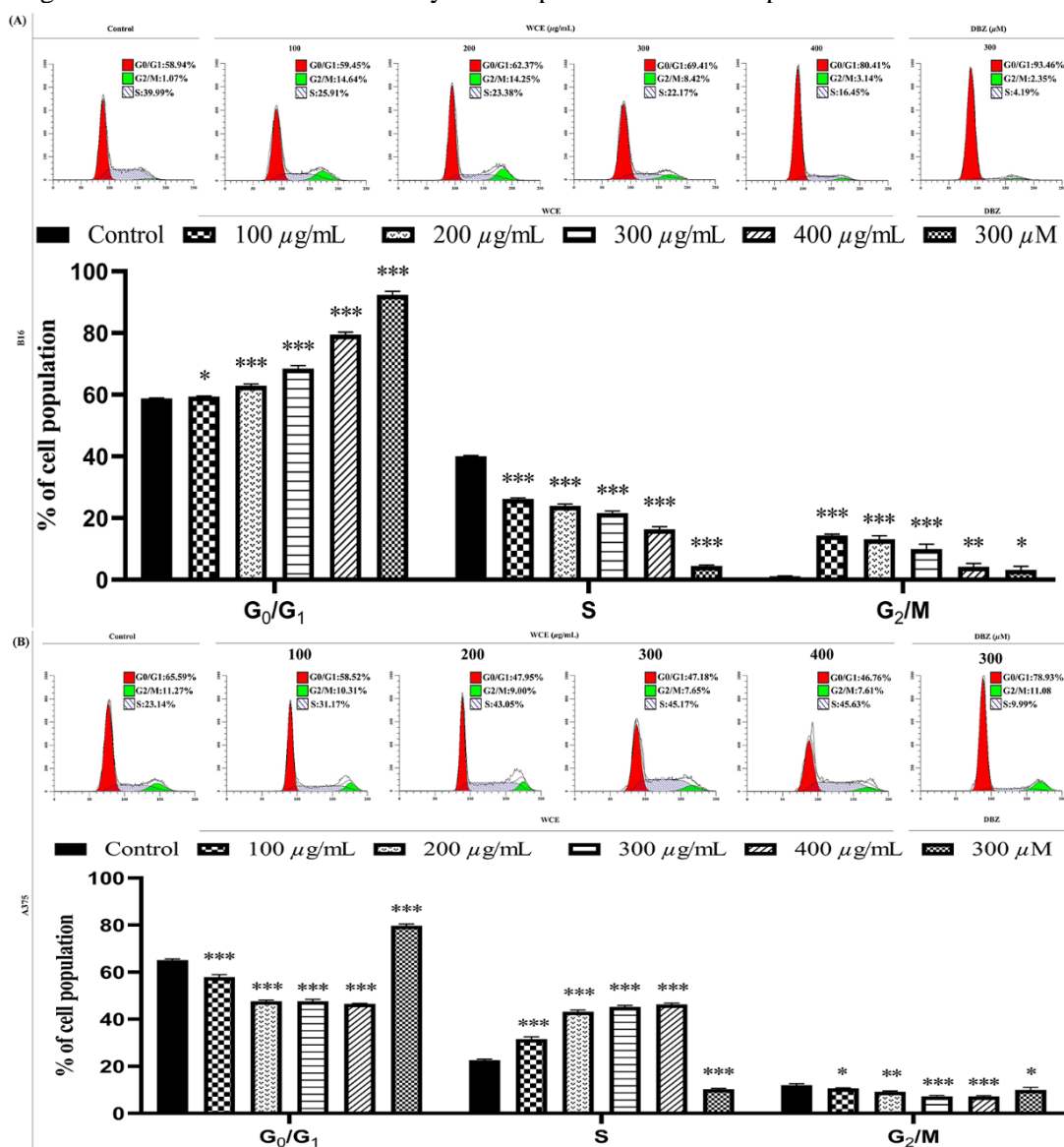

Figure 4. Effects of WCE and DBZ on cell cycle distribution. (A) WCE triggered cell cycle arrest at the G_0/G_1 phase in B16 cells. (B) WCE triggered cell cycle arrest at the S phase in A375 cells. B16 and A375 cells were treated for 24 hours. The cells were then harvested, stained with PI, and analyzed using flow cytometry. Following flow cytometry analysis, the Mod Fit LT 5.1 software was used to calculate the frequencies of cells in each phase of the cell cycle. *p < 0.05, **p < 0.01, and ***p < 0.001 vs control group

Antitumor activity of *Wikstroemia chamaedaphne*

3.5. The WCE Induce Apoptosis in B16 and A375 Melanoma Cells

The percentage of apoptotic cells was determined using flow cytometry and Annexin V-FITC/PI double staining. As shown in Figure 5, cells considered viable were annexin V-FITC and PI negative, cells in early apoptosis were annexin V-FITC positive and PI negative, and cells in late apoptosis or already dead were both annexin V-FITC and PI positive. The percentages of total apoptotic cells in B16 were 27.35 %, 45.38%, 69.18%, and 81.03% after 24 hours of treatment with 100, 200, 300, and 400 μg/mL, respectively, and the percentages of total apoptotic cells in A375 were 36.54%, 53.26%, 70.59%, and 74.81 %. These findings revealed that WCE induced apoptosis in B16 and A375 cells was dose-dependent.
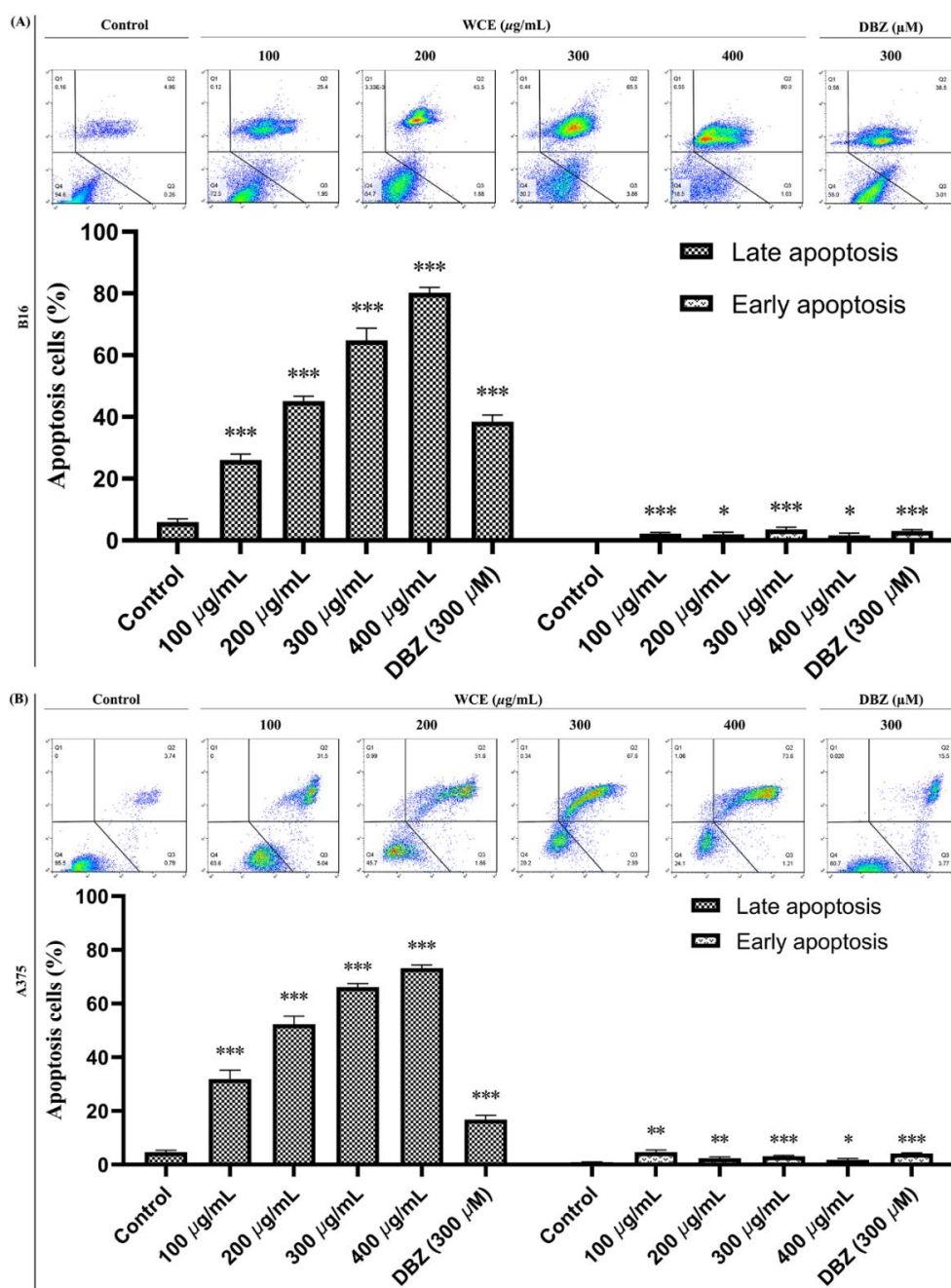

Figure 5. Apoptosis in A375 and B16 cells induced by WCE and DBZ. (A) A375 cells were treated with different concentration of WCE and DBZ for 24 h. (B) B16 cells were treated with different concentration of WCE and DBZ for 24 h. $*p < 0.05$, $**p < 0.01$, and $***p < 0.001$ vs control group

567

Li *et.al.*, *Rec. Nat. Prod.* (2022) 16:6 559-571

3.6. Phytochemical Screening of WCE

The phytochemical investigation of *W. chamaedaphne* extract led to isolation of five flavonoids (**1–5**) and three diterpenoids (**6–8**), including a new tigliane-type diterpenoid wikstchalin A (**6**) (Figure 6). The known compounds were identified as isoquercitrin (**1**) [10], eriodictyol (**2**) [11], luteolin (**3**) [12], apigenin (**4**) [13], diosmetin (**5**) [14], pimelotide A (**7**) [15], $6\alpha,7\alpha$-epoxy-5β-hydroxy-12-deoxyphorbol-13-decanoate (**8**) [16]. The absolute structure of pimelotide A (**7**) were determined by single-crystal X-ray diffraction (Figure 7). We estimated that WCE contained highly amount of isoquercitrin (11.1%), eriodictyol (2.8%), luteolin (44.4%), apigenin (0.9%), diosmetin (1.7%), wikstchalin A (0.43%), pimelotide A (0.53%), and $6\alpha,7\alpha$-epoxy-5β-hydroxy-12-deoxyphorbol-13-decanoate (0.26%) (Figure 8).
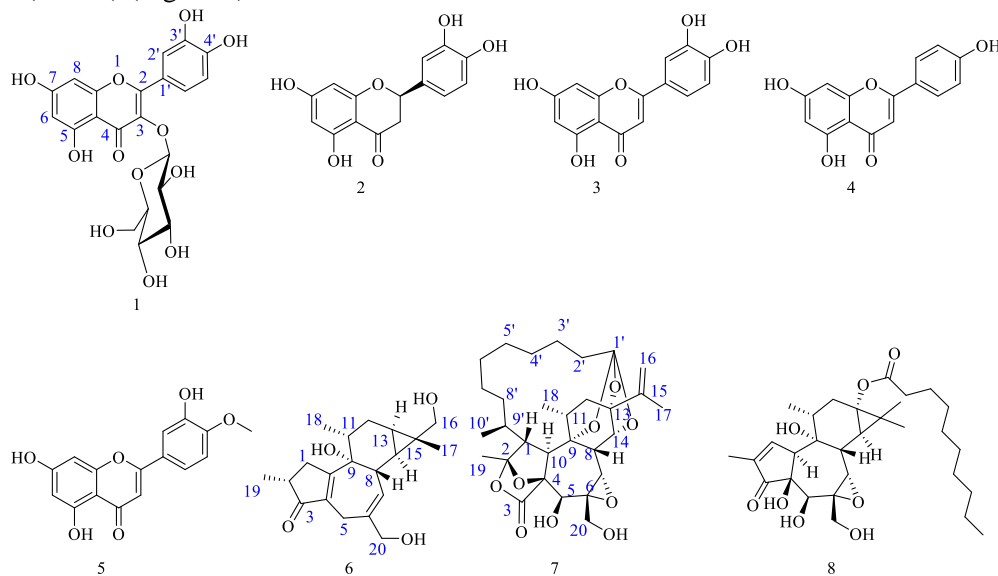

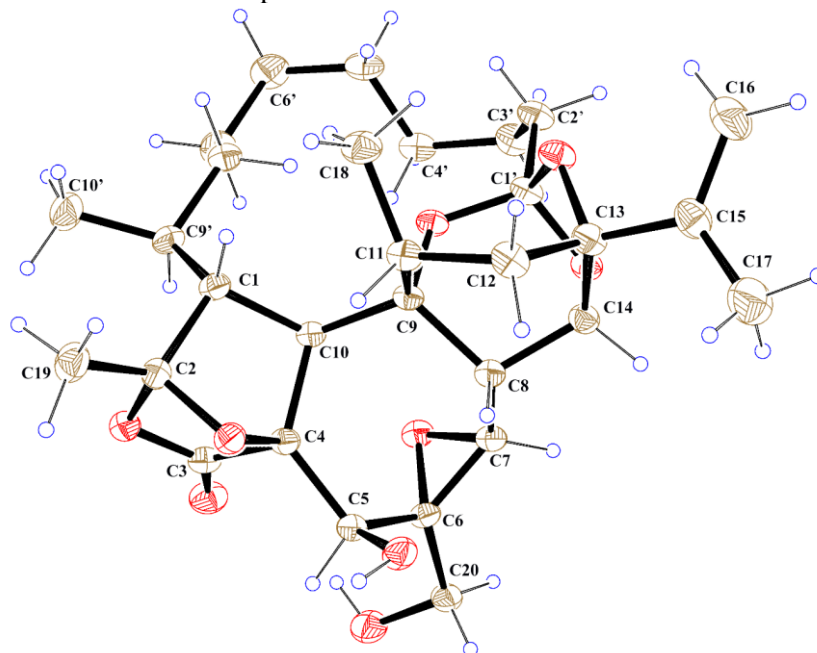**Figure 6**. Structures of compounds **1−8** isolated from *Wikstroemia chamaedaphne*
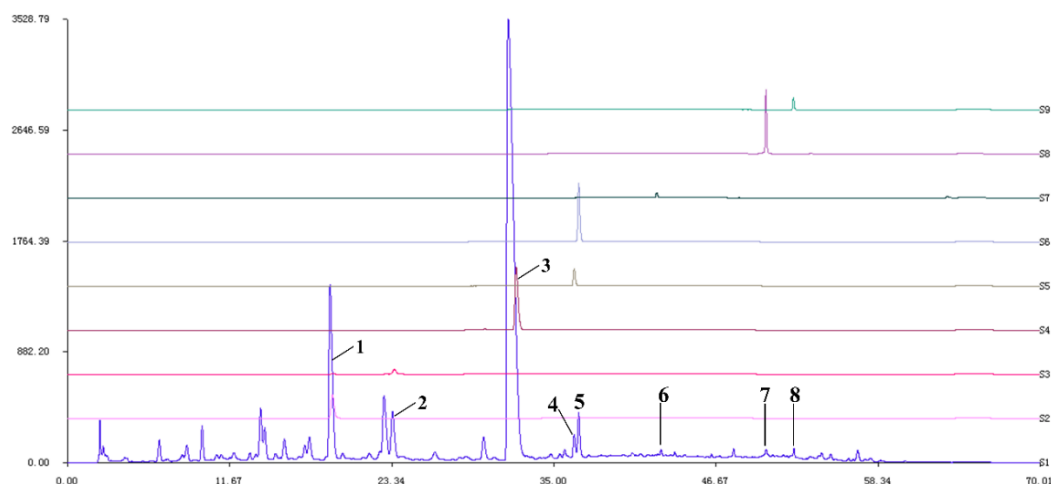

Figure 7. ORTEP diagram of pimelotide A (**7**)

Figure 8. 1: isoquercitrin; 2: eriodictyol; 3: luteolin; 4: apigenin; 5: diosmetin; 6: wikstchalin A; 7: pimelotide A; 8: $6\alpha,7\alpha$-epoxy-5β-hydroxy-12-deoxyphorbol-13-decanoate

3.7. Structural Identification of New Compound Wikstchalin A

Compound **6**, a white powder, had the molecular formula $C_{20}H_{28}O_4$, as determined by HRESIMS at m/z 331.1926 [M − H]⁻ (calcd for $C_{20}H_{27}O_4$, 331.1915), indicating to seven degrees of unsaturation. The IR spectrum exhibited absorption bands for hydroxyl (3364 cm^{-1}) and α,β-unsaturated ketone groups (1698 and 1681 cm^{-1}) functionalities. The ^{1}H NMR spectrum (Table 1) of **6** showed one methyl singlet and two dublets [δ_H 1.23 (3H, s, CH$_3$-17), 1.22 (3H, d, J = 6.2 Hz, CH$_3$-18), and 1.20 (3H, d, J = 4.4 Hz, CH$_3$-19)], one aromatic protons δ_H 5.64 (1H, d, J = 7.3 Hz, H-7), and a series of aliphatic methylene multiplets. In combination with DEPT experiments, the ^{13}C NMR spectrum (Table 1) experiments resolved 20 carbon resonances attributable to a ketone group (δ_C 211.1), two double bonds (δ_C 167.4, 140.8, 134.5, and 128.2), two sp^3 quaternary carbons (one oxygenated), five sp^3 methines, five sp^3 methylenes (two oxygenated), and three methyls. Since a ketone and two double bonds accounted for three of the seven degrees of unsaturation, the remaining degrees of unsaturation required that compound **6** be a tetracyclic system. According to the data presented above, **6** possessed the majority of the structural features of tigliane diterpenoids, which were strikingly similar to those of stracheyioid A [17]. In comparison with stracheyioid A, the major differences being the double bond between C-1 and C-2 in stracheyioid A was instead by the double bond between C-4 and C-10 in **6**. The location of the $\Delta^{4(10)}$ was assigned between C-4 and C-10 by HMBC correlations from H$_2$-1 to C-4 (δ_C 134.5) and C-10 (δ_C 167.4), and from H$_2$-5 to C-4 and C-10. Detail analyses of **6**'s 2D NMR data further confirmed its planar structure (Figure 9A). The relative configuration of **6** was determined using the NOESY experiment and comparing its 1D NMR data to that of stracheyioid A. The NOE interactions of H-13/H-14 indicated that the dimethyl cyclopropane was cis-oriented and was arbitrarily assigned as β. The NOE interactions (Figure 9B) of H-7/Hα-5, H-7/H-14, H-14/H-13, and H$_2$-16/H-14 suggested that H-13, H$_3$-14, and H$_2$-16 were cofacial and were assigned to be α-oriented randomly. H$_3$-18/Hα-1, H$_3$-16/Hα-1, H-11/H-8, and H-14/H$_3$-17 assigned H-2, H-11, H-8, and H$_3$-17 as β. The absolute configuration of **6** was established by CD exciton chirality method [18]. The CD spectrum of **6** exhibited negative chirality due to exciton coupling of a nondegenerate system containing two different chromophores of the the α,β-unsaturated ketone at 235 nm (Δε −5.61, $\pi \rightarrow \pi^*$ transition) and the $\Delta^{4(10)}$ double bond at 195 nm (Δε +18.15, $\pi \rightarrow \pi^*$ transition). The negative chirality of **6** revealed that the transition dipole moments of two chromophores were oriented in a counterclockwise manner (Figure 10), and the absolute stereochemistry of **6** was assigned. Therefore, compound **6** was given a trivial name wikstchalin A.

Table 1. ^{1}H NMR (600 MHz) and^{13}C NMR (150 MHz) data of compound **6** in CDCl$_3$ (δ_C in ppm, *J* in Hz).

No.	δ_H	δ_C	No.	δ_H	δ_C
1a	2.70, dd (18.4, 6.5)	37.7, CH$_2$	12a	2.57, d (11.2)	32.6, CH$_2$
1b	2.50, m		12b	1.55, d (3.9)	
2	2.46, m	39.0, CH	13	1.53, s	26.5, CH
3		211.1, C	14	1.32, d (12.6)	34.2, CH
4		134.5, C	15		31.3, C
5	2.94, 2H, s	22.9, CH$_2$	16	3.34, 2H, d (4.4)	71.5, CH$_2$
6		140.8, C	17	1.23, s	10.8, CH$_3$
7	5.64, d (7.3)	128.2, CH	18	1.22, s	20.3, CH$_3$
8	2.83, m	43.4, CH	19	1.20, d (4.4)	16.6, CH$_3$
9		70.5, C	20a	4.16, d (13.2)	67.2, CH$_2$
10		167.4, C	20b	4.03, d (13.2)	
11	2.52, m	37.3, CH			
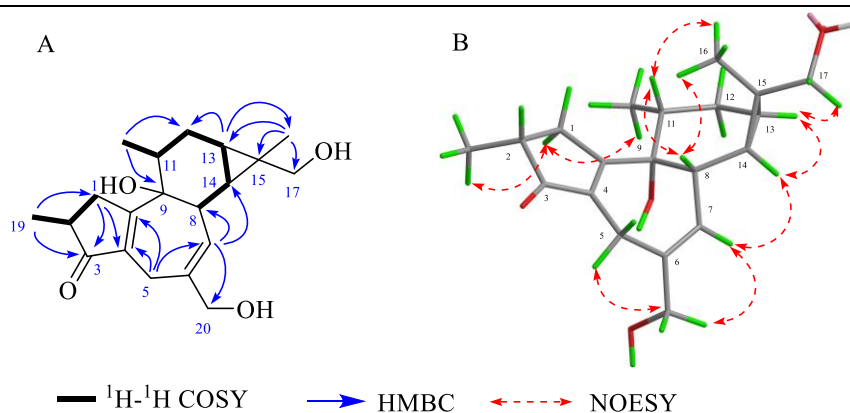
Figure 9. The 2D NMR correlations of **6** (A) Key ^{1}H–^{1}H COSY and HMBC of **6**. (B) Selected NOESY correlations of **6**
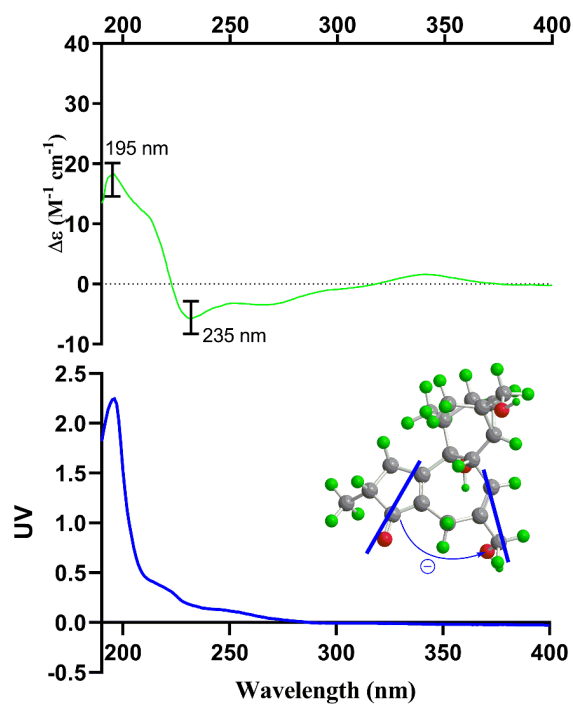
Figure 10. CD and UV spectra of **6** (Line arrow denote the electric transition dipole of the chromophores)

Antitumor activity of *Wikstroemia chamaedaphne*

3.8. Cytotoxic Effects of the Isolates

The MTT assay was used to assess the *in vitro* cytotoxicity of all isolated compounds **1−8** against B16 cell lines. Compound **8** was discovered to be the most active compound, with an IC_{50} value of 7.9 μM, compared to the positive control DBZ against B16, which had an IC_{50} value of 300 μM.

4. Conclusion

The WCE was found to be highly cytotoxic to the melanoma cell lines B16 and A375, with IC_{50} values of 156.2 and 192.8 μg/mL, respectively. In an acridine orange and propidium iodide (AO/PI) staining assay, WCE-treated B16 and A375 cells showed typical morphological changes of cell apoptosis. To assess cell migration, a wound healing assay was used. WCE induced cell cycle arrest at the G_0/G_1 phase in B16 cells and the S phase in A375 cells, according to cell cycle analysis with propidium iodide staining. WCE induced apoptotic events in B16 and A375 cells in a dose-dependent manner, according to flow cytometric analysis using Annexin V-FITC and propidium iodide staining. These findings strongly suggested that WCE could be developed further as a potential antitumor agent. Chemical analysis of the WCE resulted in the isolation of a new wikstchalin A (**6**), in addition to the five known flavonoids (**1–5**) and two known diterpenoids (**7** and **8**). Single-crystal X-ray diffraction was used to confirm one of the diterpenoids, pimelotide A (**7**). All compounds were tested for cytotoxicity against the B16 cell line, and compound **8** inhibited B16 with an IC_{50} values of 7.9 μM, making it more active than the positive control, DBZ (IC_{50} = 300 μM). However, the mechanism of compound **8**'s inhibition of B16 cell line proliferation requires further investigation.

Supporting Information

Supporting information accompanies this paper on http://www.acgpubs.org/journal/records-of-natural-products

ORCID
Yuan Li: 0000-0002-6498-5393
Chunyan Zhang: 0000-0002-5410-1048
Yiwen Nie: 0000-0001-6478-4770
Ruifeng Zhang: 0000-0003-1251-5725
Xiaoxiang Zhai: 0000-0003-1527-1236
Yanjuan Duan: 0000-0003-1995-8449
Wei Fan: 0000-0002-7980-0005
Weiying Gu: 0000-0003-1559-1575
Kourong Shi: 0000-0002-1531-9183
Lan Luo: 0000-0003-2364-6384
Jianyong Zhu: 0000-0001-5922-9326

References

[1]   D. Schadendorf, A. Akkooi, C. Berking, K.G. Griewank, R. Gutzmer, A. Hauschild, A. Stang, A. Roesch and S. Ugurel (2018). Melanoma, *The Lancet.* **392**, 971-984.

[2]   W. Sun and L.M. Schuchter (2001). Metastatic melanoma, *Curr.Treat. Option. On.* **2**,193-202.

[3]   Z.Q. Zhang, S.F. Li, L.W. Zhang and J.B. Chao (2017). Chemical constituents from flowers of *Wikstroemia chamaedaphne* and their anti-hepatitis B virus activity, *Chin. Trad. Herb. Drugs*. **48**, 1292-1297.

[4]   S.F. Li, Y.Y. Jiao, Z.Q. Zhang, J.B. Chao, J. Jia, X.L. Shi and L.W. Zhang (2018). Diterpenes from buds of *Wikstroemia chamaedaphne* showing anti-hepatitis B virus activities, *Phytochemistry* **151**,17-25.

[5]   J.R. Guo, J. Tian, G.M. Yao, H.C. Zhu, Y.B. Xue, Z.W. Luo, J.W. Zhang, Y. Zhang and Y.H. Zhang (2015), Three new 1α-alkyldaphnane-type diterpenoids from the flower buds of *Wikstroemia chamaedaphne*, *Fitoterapia* **106**, 242-246.

[6]   J.R. Guo, J.W. Zhang, P.H. Shu, L.M. Kong, X.C. Hao, Y.B. Xue, Z.W. Luo, Y. Li, G. Li, G.M. Yao and Y.H. Zhang (2012), Two new diterpenoids from the buds of *Wikstroemia chamaedaphne*, *Molecules* **17**, 6424-6433.

[7]   X. Liang, Y.Y. Jiao, W.H. Wang, S.F. Li and L.W. Zhang (2019), Phenolic constituents from *Wikstroemia chamaedaphne*, *Chin. J. Chin. Mater. Med*. **44**, 962-967.

[8]   R.R. Pan, C.Y. Zhang, Y. Li, B.B. Zhang, L. Zhao, Y. Ye, Y.N. Song, M. Zhang, H.Y. Tie, H. Zhang and J.Y. Zhu (2020), Daphnane diterpenoids from *Daphne genkwa* inhibit PI3K/Akt/mTOR signaling and induce cell cycle arrest and apoptosis in human colon cancer cells, *J. Nat. Prod*. **83**, 1238-1248.

[9]   C.Y. Zhang, L.J. Zhang, Z.C. Lu, C.Y. Ma, Y. Ye, K. Rahman, H. Zhang and J.Y. Zhu (2018). Antitumor activity of diterpenoids from *Jatropha gossypiifolia*: Cell cycle arrest and apoptosis-inducing activity in RKO colon cancer cells, *J. Nat. Prod*. **81**, 1701-1710.

[10]   J. Han, M. Bang, O. Chun, D. Kim, C. Lee and N. Baek (2004). Flavonol glycosides from the aerial parts of *Aceriphyllum rossii* and their antioxidant activities, *Arch. Pharm. Res*. **27**,390-395.

[11]   S. Nakashima, H. Matsuda, Y. Oda, S. Nakamura, F. Xu and M. Yoshikawa (2010). Melanogenesis inhibitors from the desert plant *Anastatica hierochuntica* in B16 melanoma cells, *Bioorg. Med. Chem.***18**, 2337-2345.

[12]   D. Youssef and A.W.Frahm (1995). Constituents of the Egyptian *Centaurea scoparia*. III. Phenolic constituents of the aerial parts, *Planta Med*. **61**, 570-573.

[13]   W. Li, R.J. Dai, Y.H. Yu, L. Li, C.M. Wu, W.W. Luan, W.W. Meng, X.S. Zhang and Y.L. Deng (2007). Antihyperglycemic effect of *Cephalotaxus sinensis* leaves and GLUT-4 translocation facilitating activity of its flavonoid constituents, *Biol. Pharm. Bull*. **30**, 1123-1129.

[14]   Y.L. Zhang, Z.Y. Feng and X.K. Zheng (2014). Chemical constituents from the leaves of *Rehmannia glutinosa Libosch*, *J. Pharm. Sci*. **49**, 15-21.

[15]   P.Y. Hayes, S. Chow, M.J. Somerville, J.J.D. Voss and M.T. Fletcher (2009), Pimelotides A and B, diterpenoid ketal-lactone orthoesters with an unprecedented skeleton from *Pimelea elongate*, *J. Nat. Prod.***72**, 2081-2083.

[16]   P.Y. Hayes, S. Chow, M.J. Somerville, M.T. Fletcher and J.J.D Voss (2010). Daphnane and tigliane-type diterpenoid esters and orthoesters from *Pimelea elongate*, *J. Nat. Prod.***73**, 1907-1913.

[17]   D.S. Yang, W.B. Peng, Z.L. Li, X. Wang, J.G. Wei, Q.X. He, Y.P. Yang, K.C. Liu and X.L. Li (2014). Chemical constituents from *Euphorbia stracheyi* and their biological activities, *Fitoterapia* **97**, 211-218.

[18]   X.N. Wang, S. Yin, C.Q. Fan, F.D. Wang, L.P. Lin, J. Ding and J.M. Yue (2006). Turrapubesins A and B, first examples of halogenated and maleimide-bearing limonoids in nature from *Turraea pubescens*, *Org. Lett.* **8**, 3845-3848.